Synthesis of Bi-substrate State Mimics of Dihydropteroate Synthase as Potential Inhibitors and Molecular Probes

Jianjun Qi[1], **Kristopher G. Virga**[1], **Sourav Das**[2], **Ying Zhao**[2], **Mi-Kyung Yun**[3], **Stephen W. White**[3], and **Richard E. Lee**[1,2,*]

[1] Department of Pharmaceutical Sciences, University of Tennessee Health Science Center, 847 Monroe Ave Rm327, Memphis, TN 38613

[2] Department of Chemical Biology and Therapeutics, St. Jude Children's Research Hospital, 262 Danny Thomas Place, Mail stop 1000, Memphis, TN 38105-3678

[3] Department of Structural Biology, St. Jude Children's Research Hospital, 332 N. Lauderdale, Memphis, TN 38105

Abstract

The increasing emergence of resistant bacteria drives us to design and develop new antimicrobial agents. Pursuant to that goal, a new targeting approach of the dihydropteroate synthase enzyme, which serves as the site of action for the sulfonamide class of antimicrobial agents, is being explored. Using structural information, a new class of transition state mimics has been designed and synthesized that have the capacity to bind to the pterin, phosphate and para-amino binding sites. The design, synthesis and evaluation of these compounds as inhibitors of *Bacillus anthracis* dihydropteroate synthase is described herein. Outcomes from this work have identified the first trivalent inhibitors of dihydropteroate synthase whose activity displayed slow binding inhibition. The most active compounds in this series contained an oxidized pterin ring. The binding of these inhibitors was modeled into the dihydropteroate synthase active site and demonstrated a good correlation with the observed bioassay data, as well as provided important insight for the future design of higher affinity transition state mimics.

Keywords

dihydropteroate synthase; antimicrobial agent; sulfonamide; transition state analog

Introduction

Dihydropteroate synthase (DHPS) has been a validated drug target for antimicrobial therapy for over 70 years.[1] DHPS is the target enzyme of the sulfonamide class of antimicrobial agents. Currently, sulfonamides are most commonly used in combination with the dihydrofolate reductase (DHFR) inhibitor, Trimethoprim. These combination therapies are typically reserved for the treatment of complicated urinary tract infections, *Pneumocystis carinii* infections in immune-compromised patients, and as one of the few orally available treatments for community acquired methicillin resistant *Staphylococcus aureus* (MRSA).

---

[*]To whom the correspondence should be addressed. Richard.lee@stjude.org. Phone: 901 595 6617. Fax: 901 595 5715.

DHPS (*FolP*) catalyzes the fifth step in the folate biosynthesis pathway and is also the point of convergence of the two enzyme pathways making it an excellent target for therapeutic intervention. DHPS is responsible for the formation of the folate intermediate 7,8-dihydropteroic acid from *p*-aminobenzoic acid (*p*ABA) and dihydropterin-6-hydroxymethyl pyrophosphate (DHPP) (Figure 1). The sulfonamides act as competitive inhibitors with respect to the *p*-amino benzoic acid (*p*ABA) substrate within the DHPS enzyme active site. [2−4] The *p*ABA/sulfonamide binding site is formed close to the protein surface by flexible protein loops that are amenable and tolerant to mutations, thus explaining the rapid development of sulfonamide resistance found clinically. To overcome this problem, we have focused our efforts towards investigating inhibitors designed to target the conserved central pterin binding site within DHPS. [3, 5−6]

In this study, we have further expanded our approach to examine the potential of generating transition state inhibitors that simultaneously contact the pterin, *p*ABA and pyrophosphate binding sites. The use of transition state analogs is a well-established medicinal chemistry method to develop potent enzyme inhibitors and has lead to the development of such drugs as the HIV protease inhibitors and the anti-influenza neuraminidase inhibitors. [7−8] It is also hoped that the development of DHPS transition state analogs may generate biological probes capable of trapping the flexible loops, 1 and 2, which harbors mutational sites associated with sulfadrug resistance and form the *p*ABA binding site such that they may be crystallized in their active conformation. Resolution of the active conformation is a highly significant outcome, as it will facilitate future structure-based drug design efforts of novel DHPS inhibitors, but also to further elucidate the mode of sulfonamide resistance. The belief that transition state analogs can be successfully developed lies in the fact that although the enzymatic catalytic mechanism of DHPS is poorly understood, the actual chemical reaction that takes place is relatively straightforward.

The reaction catalyzed by DHPS involves a nucleophilic attack by the amino nitrogen of *p*ABA on the exocyclic methyl carbon of DHPP. This results in the formation of the N-C bond and the elimination of the pyrophosphate moiety as a leaving group (Figure 1). As seen in Figure 1 (the proposed transition state) a partial carbocation intermediate is believed to form at the extra-cyclic methylene in the transition state, which is stabilized by delocalization of the charge in the adjacent double bond of the pterin ring. Evidence supporting transient carbocation intermediate is shown by the inability of the oxidized form of DHPP (pterin-6-hydroxymethyl pyrophosphate) to act as a DHPS substrate. The absolute geometry of the enzyme catalyzed reaction is still a matter of speculation, as it has not been defined in the available crystal structures. However, it is reasonable to assume nucleophilic attack by pABA is probably in-line with respect to the pyrophosphate moiety to facilitate its removal. The pyrophosphate is presumably anchored by a divalent cation that occupies the phosphate binding site. [9] Based on this proposed transition state, four stable transition state analogs were designed to have the ability and conformational flexibility to bind the pterin, *p*ABA, and phosphate sites within DHPS simultaneously (Figure 1). Integral to the design of these analogs was the ability to mimic the intermediate transient carbocation by the incorporation of a basic amine at the 6-position of the pterin ring, which is a similar approach that has successfully been applied to design of transition state inhibitors of purine nucleoside phorphorylase and to various glycosidase enzymes. [10−11] The inhibitors were also designed with three additional changes from the transition state theorized. For reasons of chemical stability the 5 position nitrogen in the pterin ring was removed. A methylene spacer was introduced between the pABA mimic and the 6-position exocyclic nitrogen allowing the pABA mimic greater flexibility to better fit our design model. Finally methylene spaced phosphonates of two lengths were designed to introduce a stable phosphate mimic capable of interacting with the pyrophosphate binding pocket.

Chemistry

The initial stage of the synthesis required the actual construction of the stabilized 5-deaza pterin ring lacking the nitrogen atom at the 5 position to allow for the introduction of an amino group at the 6 position. This core 2-amino-3,4-dihydro-4-oxo-6-nitropyrido[2,3-*d*]pyrimidine (**2**) was synthesized (Scheme 1) in three steps. The first step in the construction of the heterocyclic scaffold required the production of sodium nitromalonaldehyde monohydrate (**1**) from the reaction of sodium nitrite and mucobromic acid.12 This material is considered unstable and potentially explosive requiring its immediate use in the following step. The second step is a condensation reaction of the nitromalonaldehyde onto the existing heterocyclic ring scaffold of 2,4-diamino-6-hydroxypyrimidine performed in the presence of aqueous base.13 This reaction produced the fused 2-ring heterocyclic, modified 6-nitro-5-deaza pterin as a sodium salt that was converted to free amide by boiling the salt in hydrochloric acid, which afforded the product **2** as fine orange-tan needles upon cooling.

Our synthetic strategy next required the 2-amino to be protected as an amide. Initially, we explored the use of an acetyl protection scheme. However, difficulties with the organic solubility of some of the subsequent intermediates were encountered so we switched to the use of bulkier and more lipophilic pivaloyl protecting group. This had the desired effect of increasing solubility and allowed the scheme to advance. Thus, **2** was protected as a pivaloyl amide by reaction with pivaloyl anhydride to afford **3**. The nitro group in the pyrimidine ring of **3** was then reduced by catalytic hydrogenation or with iron in acetic acid to afford 6-amino-compound **4**. The next step introduced the *p*ABA mimic by reductive amination of **4** with 4-formyl-benzoic acid methyl ester in the presence of borane-*tert*-butylamine complex, which allowed the reaction to proceeded smoothly affording **5**.14

Next, the addition of the phosphate mimic was addressed. This was first attempted by direct alkylation of **5** with (2-bromo-ethyl, or propyl)-phosphonic acid diethyl ester according to the procedure of Singh.15 However, problems were encountered with this procedure. In the absence of base, the coupling reaction resulted in rapid depivaloylation of the starting material, which then precipitated out of solution blocking further reaction. A second problem was encountered when this reaction was attempted in the presence of base (Et$_3$N) to block the aforementioned pivaloyl hydrolysis; alkylation of the 4-oxo occurred as a competing reaction creating a mixture of products. Therefore, the alternative approach of reductive amination of **5** with (2-oxo-ethyl, or propyl)-phosphonic acid diethyl ester was attempted (scheme 3). In this reaction, the phosphonate aldehydes were reacted with compound **5** in AcOH overnight at RT followed by reduction of the imine intermediate by borane-*tert*-butylamine complex. Notable differences in the final yields of the desired products were obtained between the two aldehydes (**6** 56% and **7** 25% yield). This was attributed to the ability of ethyl rather than the propyl phosphonate to stabilize the intermediate β-imine.

Phosphonate deprotection of **6** and **7** with excess TMSBr in DCM at RT for 24 h gave corresponding free phosphonates **8** and **9** which were subjected to base hydrolysis to give target compounds **10** and **11**. In addition to the oxidized analogs **10** and **11,** transition state mimics in which the outer pterin-like ring was reduced were also explored, as this ring is only partially desaturated in the natural substrate. To synthetically achieve such analogs, selective hydrogenation of the outer ring of compounds **8** and **9** was achieved using compressed hydrogen and catalytic platinum oxide in TFA to give a mixture of desired outer ring saturated products. These acidic reaction conditions also produced some of the depivaloylation product. Rather than attempt purification at this stage, the product mixture was advanced directly onto the next synthetic step; removal of the remaining pivaloyl and

ester functionalities via base hydrolysis to afford target compounds **12** and **13 as their respective** racemic mixtures (Scheme 4).

Enzyme inhibition and molecular modeling

Compounds **10**–**13** were all tested for inhibition of *B. anthracis* DHPS using an endpoint assay and radiometric detection of the product (Table 1).6 The results showed that oxidized analogs **10** and **11** demonstrated significant DHPS inhibition, whereas the reduced analogs **12** and **13** were inactive. The lack of inhibition of the reduced analogs indicates that sp2 centers are required at the pterin 5–6 positions for inhibition. This is likely attributable to resulting steric clashes with the protein when the pterin ring at the 5–6 position is reduced and sp3 centers are introduced. The inhibition of **10** and **11** could be improved significantly by pre-incubation of the inhibitor before the addition of the DHPP substrate suggesting slow binding kinetics. As could be expected from the level of inhibition, none of the compounds demonstrated significant antimicrobial activity when tested against a panel of gram positive organisms including *B. anthracis*.

The poor solubility and low affinity of these compounds in our crystallization conditions prevented the soaking or co-crystallization these molecules with BaDHPS. Therefore, molecular modeling experiments were performed using our established and validated model of the BaDHPS active site in an effort to rationalize our resutls.5 All the inhibitors were docked into the active site using GlideXP module of Maestro from Schrodinger Inc.16 The scores obtained are shown in Table 2. As anticipated, the docking scores followed a similar trend to the observed inhibition of the inhibitors. The reduced analog **13** had poor docking scores mirroring its observed poor enzyme inhibition. **11** had the highest docking score, also mirroring the observed biological activity. Consequently, **11** was redocked into BaDHPS for exploring the possibility of alternate binding modes. The best docked complex, which was similar to that obtained in the previous docking exercise with the exception of the phosphonate-protein interactions, was further subjected to a molecular dynamics simulation of 1 ns duration in order to probe the interaction stabilities. Figure 2c, which is a snapshot of the system at 1 ns, shows a set of stable interactions between the inhibitor and the protein. These interactions, as well as their differences from the binding modes of the substrate DHPP and product pteroic acid, are discussed below.

The transition state analog **11** lacks the nitrogen in the 5 position of the pterin ring, which has been removed to maintain chemical stability. As evidenced in Figures 2a and 2b, the absence of the 5-position nitrogen prevents the formation of a key hydrogen bond interaction between the 5-position nitrogen, the 3-position keto, and Lys220. Lys220 instead forms a hydrogen bond with the phosphonate group of **11**. The pterin mimic portion of the analog retains its interaction with Asn120. Although, only one of the two interactions of Asn120 is visible in the snapshot in Figure 2c, both interactions are observed during the course of the simulation. However, Asp184 only interacts with one of the two nitrogens. The conserved water molecule interacts with the other nitrogen during the course of the simulation, although this interaction is not visible in Figure 2c. The second difference noted was with respect to the pyrophosphate binding site that hydrogen bonded via the Arg68 and Asn27 in Figure 2c. Equivalent interactions are not present in either Figure 2a or 2b. On the other hand, Arg254 forms hydrogen bonding interactions with the phosphonate in 2c, similar to those in Figures 2a and 2b. The third difference relates to carboxylate binding site of the *p*ABA group. The carboxylate group of the *p*ABA-mimic portion of **11** hydrogen bonds with Phe222, Ala190 and Phe189. It is close to 90 degrees to the pterin-mimic portion of **11**. This conformation is different from the slightly stretched conformation adopted by pteroic acid in 1tx0 (Figure 2b), in which the carboxylate group hydrogen bonds with Ser221 instead.

Conclusions

Herein we describe the design and synthesis of the first known trivalent DHPS inhibitors. The inhibitors appear to demonstrate slow binding inhibition, which is consistent with the rearrangement of the active site to bind these large transition-state mimics. This may also bode well for future inhibitor design as slow K_{off} rates have been shown to be important in the action of several inhibitor classes.[17] If designed well, transition-state mimic inhibitors should have nanomolar inhibition. Thus, there is still much room to improve the design of these inhibitors. From the modeling experiments, it is clear that there are 3 interactions missing in our transition-state mimics that are found in the substrate, the product and presumably, in the transition state with DHPS. If these interactions can be addressed, most notably the inclusion of a hydrogen bond acceptor at the 5 position of the pterin ring and an increase in the distance between the pterin and *p*ABA mimic rings, then we would predict higher affinity inhibitors will be obtained. A further consideration in the design that needs to be incorporated is the degree of S_N2 vs S_N1 character in the enzyme reaction. Finally, as satisfactory aqueous solubility will be required for the development of such inhibitors towards drugs, future inhibitor designs must address the poor solubility in aqueous and organic media of such pterin like systems resulting from their high crystal lattice energies.

Experimental section

The reactions were monitored by thin layer chromatography (TLC) on pre-coated Merck 60 F254 silica gel plates and visualized by UV detection. Horizon HPFC flash chromatography system was performed with Biotage silica gel cartridges, Biotage Inc. (Lake Forest, VA). HPLC on a Gilson 215 HPLC (Middleton, WI) equipped with an Xterra® Prep MS C18 5 μm, 19×100 mm column (Milford, MA); gradient MeCN/H_2O 0.1% TFA, 0 to 100% (30 min) with dual wavelength detection at 215 and 254 nm. Analytical HPLC analysis were performed on a Bruker Esquire LC/MS equipped with an Alltech Platinum EPS 5 μm C18, 4.6×150 mm column (Deerfield, IL); gradient MeCN/H_2O 0.1% TFA, 0 to 100% (22 min) with detection at 254 nm. All compounds were determined to be of acceptable purity (>95%) using this method. Melting points were obtained on a Thomas Scientific Uni-melt capillary m.p. apparatus (Swedesboro, NJ) and were uncorrected. All ^{1}H, ^{13}C NMR and 2-D NMR spectra were recorded on a Bruker ARX-300 or Varian INOVA-500 spectrometers. Chemical shifts are reported in ppm (δ) relative to residual solvent peak or internal standard (tetramethylsilane) and coupling constants (*J*) are reported in hertz (Hz). Mass spectra were recorded on a Bruker Esquire LC/MS using ESI (Billerica, MA).

Sodium nitromalonaldehyde monohydrate (1)

To a solution of $NaNO_2$ (33.00 g, 0.48 mol) in water (33 mL) was dropwise added a solution of mucobromic acid (33.00 g, 0.13 mol) in 95% ethanol at 53~55°C about 1 h and kept stirring for 15 min at the same temperature. The reaction was cooled to 0°C and filtered. The crude product was recrystallized from a solution of 95% ethanol (50 mL) and water (12 mL) to give **1** (7.25 g, 36.3%).

2-Amino-6-nitro-3*H*-pyrido[2,3-*d*]pyrimidin-4-one (2)

A mixture of 2,4-diamino-6-hydroxypyrimidine (5.78 g, 45.86 mmol) and **1** (7.20 g, 45.86 mmol) in 46 mL of NaOH (1% aq) was refluxed vigorously for 1 h. On chilling to 50°C, a voluminous mass of yellow needles separated. The solid was recrystallized from 400 mL of 20% hydrochloric acid to give **2** (5.40 g, 57%) as green-tan needles. M.p. >300°C; ^{1}H NMR (300 MHz, DMSO-d$_6$) δ 9.39 (d, 1 H, *J* = 2.7 Hz), 8.78 (d, 1 H, *J* =2.7 Hz), 8.60~6.80 (br, 2 H). ^{13}C NMR (75 MHz, DMSO-d$_6$) δ 163.5, 161.6, 156.1, 150.6, 138.0, 130.9, 110.5; *m/z* 206 (M$^-$).

2,2-Dimethyl-*N*-(6-nitro-4-oxo-3,4-dihydro-pyrido[2,3-*d*]pyrimidin-2-yl)-propionamide (3)

A mixture of **2** (2.00 g, 9.66 mmol), 4-dimethylaminopyridine (DMAP, 0.20 g) and trimethylacetic anhydride (10 mL) was heated at reflux vigorously for 6 h. The mixture was cooled to 0°C, diluted with ether and then filtered. The crude product was dissolved in chloroform and filtered. The filtrate was concentrated to a small volume, cooled to 0°C, filtered and washed with chloroform to give **3** as a pale yellow crystal (2.09 g, 74%). TLC (ethyl acetate) R_f = 0.71; m.p. 208–210°C; ^{1}H NMR (500 MHz, DMSO-d$_6$) δ 12.76-12.22 (br, 1 H), 12-11.5 (br, 1 H), 9.56 (d, 1 H, *J* = 3.0 Hz), 8.93 (d, 1 H, *J* = 3.0Hz), 1.28 (s, 9 H). ^{13}C NMR (75 MHz, CDCl$_3$) δ 180.5, 159.0, 151.1, 150.8, 140.5, 132.0, 114.0, 40.2, 26.3; *m/z* 290 (M$^-$)

N-(6-Amino-4-oxo-3,4-dihydro-pyrido[2,3-*d*]pyrimidin-2-yl)-2,2-dimethyl-propionamide (4)

Method A—A solution of **3** (0.1 g, 0.34 mmol) in 2-methoxy-ethanol (20 mL) was charged with 5% Pd-C (0.02 g) and hydrogenated at 50 Psi for 3 h at room temperature. The reaction solution was filtered and the filtrate was evaporated to give **4** as a yellow solid (0.081 g, yield 90%). TLC (ethyl acetate) R_f = 0.1; ^{1}H NMR (500 MHz, DMSO-d$_6$) δ 12.11 (s, 1 H), 11.06 (s, 1 H), 8.32 (d, 1 H, *J* = 3.0 Hz), 7.46 (d, 1 H, *J* = 3.0 Hz), 5.69 (s, 2 H), 1.24 (s, 9 H). ^{13}C NMR (75 MHz, DMSO-d$_6$) δ 181.4, 161.3, 145.8, 144.5, 142.9, 115.0, 114.5, 79.1, 48.5, 26.3; *m/z* 284 (M$^+$+Na).

Method B—Fe-powder (0.5 g, 8.93mmol) was added to a flask, followed by water (5 mL) and EtOH (10 mL) at about 50~55°C, then 2~3 drop of HOAc was added and kept stirring for 5 min. A mixture of **3** (0.5 g, 1.72 mmol) in EtOH (5 mL) was added to the reaction flask. The mixture was stirred at 50~55°C for 1 h and cooled to room temperature, extracted with chloroform and filtered. The organic phase was dried with anhydrous Na$_2$SO$_4$, and then evaporated to yield **4** (0.42 g, yield 94%).

4-{[2-(2,2-Dimethyl-propionylamino)-4-oxo-3,4-dihydro-pyrido[2,3-*d*]pyrimidin-6-ylamino]-methyl}-benzoic acid methyl ester (5)

A mixture of **4** (1.075 g, 4.12 mmol), 4-formyl-benzoic acid methyl ester (0.67 g, 4.12 mmol) in AcOH (100 mL) was stirred overnight at room temperature. To the reaction solution was added borane-*tert*-butylamine complex (0.179 g, 2.0 mmol). The resulting mixture was stirred for 2 h at room temperature and evaporated. The residue was purified by chromatography using 4% MeOH in EtOAc as eluent to give **5 as** a yellow solid (0.401 g, yield 24 %). TLC (ethyl acetate) R_f = 0.18; m.p. >300°C; ^{1}H NMR (500 MHz, DMSO-d$_6$) δ 12.12 (br, 1 H), 11.08 (br, 1 H), 8.44 (d, 1 H, *J* = 2.0 Hz), 7.94 (d, 2 H, *J* = 8.0 Hz), 7.52 (d, 2 H, *J* = 8.0 Hz), 7.24 (d, 1 H, *J* = 3.5 Hz), 7.05 (t, 1 H, *J* = 6.0 Hz), 4.49 (d, 2 H, *J* = 6.0 Hz), 3.83 (s, 3 H), 1.23 (s, 9 H). ^{13}C NMR (75 MHz, CDCl$_3$) δ 179.8, 166.2, 144.0, 142.5, 141.7, 129.6, 129.0, 126.7, 115.2, 113.5, 51.6, 47.1, 39.8, 26.4; *m/z* 410 (M$^+$+H), 432 (M$^+$+Na).

4-({[2-(Diethoxy-phosphoryl)-ethyl]-[2-(2,2-dimethyl-propionylamino)-4-oxo-3,4-dihydro-pyrido[2,3-*d*]pyrimidin-6-yl]-amino}-methyl)-benzoic acid methyl ester (6)

A mixture of **5** (0.19 g, 0.46 mmol), (2-oxo-ethyl)-phosphonic acid diethyl ester (0.15 g, about 80%, 0.67 mmol) and 3Å molecular sieve (0.5 g) in AcOH (20mL) was stirred overnight at room temperature. Then borane-*tert*-butylamine complex (0.12 g) was added. The reaction solution was stirred for additional 2 h at room temperature, and then filtered. The filtrate was evaporated and then the residue was dissolved in chloroform, washed with a solution NaHCO$_3$ and brine. The organic phase was dried with anhydrous Na$_2$SO$_4$ and then evaporated. The resulting residue was purified by chromatography using 5% MeOH in AcOEt as eluent to give **6** as a yellow solid (0.15 g, yield 56%). TLC (MeOH/ethyl

acetate=1:15) R_f = 0.45. ^{1}H NMR (300 MHz, CDCl$_3$) δ 12.50-11.60 (1 H, br), 8.45 (d, 1 H, *J* = 3.0 Hz), 8.00 (d, 2 H, *J* =8.1 Hz), 7.67 (d, 1 H, *J* =3.0 Hz), 7.28 (d, 2 H, *J* = 8.4Hz), 4.71 (s, 2 H), 4.13 (m, 4 H), 3.92 (s, 3 H), 3.84 (m, 2 H), 2.15 (m, 2 H), 1.35 (t, 6 H, *J* = 6.9 Hz), 1.34 (s, 9 H); *m/z* 572 (M$^-$).

4-({[3-(Diethoxy-phosphoryl)-propyl]-[2-(2,2-dimethyl-propionylamino)-4-oxo-3,4-dihydro-pyrido[2,3-*d*]pyrimidin-6-yl]-amino}-methyl)-benzoic acid methyl ester (7)

A mixture of **5** (0.91 g, 2.22 mmol), (2-oxo-propyl)-phosphonic acid diethyl ester (1.50 g, 7.73 mmol) in AcOH (15 mL) was stirred overnight at 70~75°C. Then borane-*tert*-butylamine complex (0.024 g) was added to the reaction mixture hourly with stirring for 10 h at 70~75°C. The reaction was monitored by HPLC until there was no change for the ratio of product. The reaction solution was evaporated. The residue was dissolved with chloroform and then washed with brine. The organic phase was dried with anhydrous Na$_2$SO$_4$ and then evaporated. The resulting residue was purified by chromatography with 5% MeOH in AcOEt as eluent to give **7** (0.33 g, yield 25%). (600mg of starting material was recovered.) TLC (MeOH/ethyl acetate = 1:10), R_f = 0.3. ^{1}H NMR (500 MHz, CDCl$_3$) δ 11.96 (br, 1 H), 8.45 (s, 1 H), 8.27 (s, 1 H), 8.00 (d, 2 H, *J* = 8.0 Hz), 7.64 (d, 1 H, *J* = 3.5Hz), 7.28 (d, 2 H, *J* = 8.0 Hz), 4.70 (s, 2 H), 4.15-4.06 (m, 4 H), 3.91 (s, 3 H), 3.62 (t, 2 H, *J* = 8.0 Hz), 2.05-1.96 (m, 2 H), 1.80 (tt, 2 H, J_1 = 18.5 Hz, J_2 = 7.5 Hz), 1.33 (s, 9 H), 1.32 (t, 6 H, *J* = 7.0 Hz). ^{13}C NMR (75 MHz, CDCl$_3$) δ 180.2, 166.0, 161.1, 149.2, 145.6, 142.1, 142.0, 141.6, 129.5, 128.8, 125.9, 114.8, 114.5, 61.1, 53.7, 51.4, 51.0, 39.7, 26.2, 22.2, 19.7, 19.6, 15.9, 15.8; *m/z* 588 (M$^+$+H)

4-{[[2-(2,2-Dimethyl-propionylamino)-4-oxo-3,4-dihydro-pyrido[2,3-*d*]pyrimidin-6-yl]-(2-phosphono-ethyl)-amino]-methyl}-benzoic acid methyl ester (8)

A mixture of **6** (0.06 g,0.1 mmol) and bromo-trimethyl-silane (0.153 g, 1 mmol) in DCM (10 mL) was stirred at room temperature under nitrogen for 72 h and then quenched with MeOH (10 mL) followed by stirring for an additional 2 h. The reaction mixture was evaporated and the residue was purified by HPLC using 1% formic acid/water solution and acetonitrile to give **8** as a yellow solid (0.03 g, yield 58%). m.p. 232–234°C; ^{1}H NMR (500 MHz, CD$_3$OD) δ 8.40 (s, 1 H), 8.00 (d, 2 H, *J* = 7.8 Hz), 7.52 (d, 2 H, *J* = 7.3 Hz), 7.43 (s, 1 H), 4.51 (s, 2 H), 3.90 (s, 3 H), 2.86-2.78 (m, 2 H), 1.41-1.32 (m, 2 H), 1.33 (s, 9 H); *m/z* 518 (M$^+$+ H)

4-{[[2-(2,2-Dimethyl-propionylamino)-4-oxo-3,4-dihydro-pyrido[2,3-*d*]pyrimidin-6-yl]-(3-phosphono-propyl)-amino]-methyl}-benzoic acid methyl ester (9)

A mixture of **7** (0.12 g, 0.2 mmol) and bromo-trimethyl-silane (0.306 g, 2 mmol) in DCM (10 mL) was stirred at room temperature under nitrogen for 72 h and then quenched with MeOH (10 mL) followed by stirring for an additional 2 h. The reaction mixture was evaporated and the residue was purified by HPLC using 1% formic acid/water solution and acetonitrile to give **9** as a reddish solid (0.06 g, yield 56%). ^{1}H NMR (500 MHz, CD$_3$OD) δ 8.42 (d, 1 H, *J* = 2.9 Hz), 8.23 (d, 2 H, *J* = 2.4 Hz), 8.05 (d, 2 H, *J* = 8.1 Hz), 7.57 (d, 2 H, *J* = 8.1 Hz), 4.81 (t, 2 H, *J* = 7.3 Hz), 4.61 (s, 2 H), 3.92 (s, 3 H), 2.25 (q, 2 H, *J* = 7.3 Hz), 1.82-1.72 (m, 2 H), 1.36 (s, 9 H); *m/z* 532(M$^+$+H)

Potassium 4-{[[2-amino-4-oxo-3,4-dihydro-pyrido[2,3-*d*]pyrimidin-6-yl)-(2-phosphono-ethyl)-amino]-methyl}-benzoate (10)

A mixture of **8** (0.03 g, 0.06 mmol) and 1.5 N KOH (50 mL) in MeOH (50mL) was stirred for 72 h at room temperature. The reaction mixture was concentrated to about 5 mL volume. The reaction solution pH was adjusted to about 10 with AcOH. The solution was purified by HPLC using 1% formic acid/water solution and acetonitrile to afford **10** as the

monopotassium salt as a greenish-yellow solid (0.012 g, yield 44%). m.p. >300°C; ^{1}H NMR (500MHz, CD$_3$OD) δ 8.22 (s, 1 H), 8.04 (d, 2 H, J = 8.3 Hz), 7.50 (d, 2 H, J = 8.1 Hz), 7.43 (s, 1 H), 4.52 (s, 2 H), 2.42-2.15 (m, 2 H), 1.79-1.72 (m, 2 H); m/z 458.1 (M$^+$+K).

Potassium 4-{[(2-amino-4-oxo-3,4-dihydro-pyrido[2,3-*d*]pyrimidin-6-yl)-(3-phosphono-propyl)-amino]-methyl}-benzoate (11)

Compound **11** was synthesized as described for **10** from compound **9** (0.06 g, 0.11 mmol) and was obtained as an orange solid (0.002 g, 4% yield). m.p. >300°C; ^{1}H NMR (500MHz, CD$_3$OD) δ 8.22 (s, 1H), 8.04 (d, 2 H, J = 8.3 Hz), 7.54 (d, 2 H, J = 8.3 Hz), 7.43 (s, 1 H), 4.65 (t, 2 H, J = 7.3 Hz), 4.53 (s, 2 H), 2.21 (q, 2 H, J = 6.8 Hz), 1.80-1.70 (m, 2 H); m/z 472.1 (M + K)$^+$.

4-{[(2-Amino-4-oxo-3,4-dihydro-pyrido[2,3-*d*]pyrimidin-6-yl)-(2-phosphono-ethyl)-amino]-methyl}-benzoic acid (12)

To a solution of **8** (0.2 g, crude product) in TFA (20 mL) was added PtO$_2$ (0.1 g), then the reaction solution was hydrogenated under 50 Psi at room temperature for 18 h. To the reaction mixture was added PtO$_2$ (0.08 g), and the mixture was hydrogenated for an additional 6 h at 50 Psi at room temperature and monitored by LC-MS to ensure the completion of starting material. The reaction solution was filtered and the filtrate was evaporated. The crude product was used in the next step without further purification. To a solution of 1N NaOH (30 mL) was added the above crude product. The reaction solution was stirred at room temperature for 12 h and then adjusted to pH ~ 1. The reaction solution was purified by HPLC using 0.1% TFA in water and 0.35% TFA in acetonitrile as eluent to give **12** as a white solid (0.03 g, yield 27% from **6**). ^{1}H NMR (D$_2$O+NaOD, 500MHz) δ 7.82 (d, 2 H, J = 8.0 Hz), 7.46 (d, 2 H, J = 8.0 Hz), 3.82 (d, 2 H, J = 3.0 Hz), 3.44 (m, 1 H), 3.13 (t, 1 H, J = 11 Hz), 3.03 (m, 1H), 2.86 (m, 2H), 2.73 (m, 1H), 2.39 (dd, 1 H, J_1 = 11 Hz, J_2 = 15 Hz), 1.69 (m, 2 H); m/z 422 (M$^-$-H).

4-{[(2-Amino-4-oxo-3,4-dihydro-pyrido[2,3-*d*]pyrimidin-6-yl)-(3-phosphono-propyl)-amino]-methyl}-benzoic acid (13)

Compound **13** was synthesized as described for **12** from **7** (0.33g, 0.56mmol) and was obtained as a pale yellow solid product (yield 38% from **7**). ^{1}H NMR (500MHz, D$_2$O+ NaOD) δ 7.78 (d, 2 H, J = 8.5 Hz), 7.42 (d, 2 H, J = 8.5 Hz), 3.80 (s, 2 H), 3.40 (m, 1 H), 3.30 (s, 1 H), 3.10 (t, 1 H, J = 11 Hz), 3.06-2.98 (m, 1 H), 2.75-2.67 (m, 1 H), 2.62-2.53 (m, 2 H) 2.35 (dd, 1 H, J_1 = 15.5 Hz, J_2 = 10.5 Hz), 1.76-1.64 (m, 2 H), 1.30-1.20 (m, 2 H). ^{13}C NMR (75MHz, D$_2$O+ NaOD) δ 21.35 (d, J = 92 Hz), 26.76 (d, J = 130 Hz), 41.62, 51.02 (d, J = 21 Hz), 53.17 (d, J = 13 Hz), 85.96, 128.0, 128.40, 128.63,129.26, 134.68, 141.21, 159.85, 161.02, 173.67, 174.96; m/z 438(M$^+$+H).

Enzyme Assay—DHPS activity was measured in a 30 μL reaction containing 5 μM [14]C *p*ABA, 12.5 μM 6-Hydroxymethyl-7,8-dihydropterin diphosphate, 10 mM magnesium chloride, 2% PEG400, 4% DMSO, 50 mM HEPES pH 7.6, and 10 ng DHPS.[6, 18] After 30 minutes incubation at 37 °C, the reactions were stopped by addition of 1 μL of 50% acetic acid in an ice bath. The labeled product of the reaction, ^{14}C dihydropteroate, was separated from [14]C *p*ABA by thin layer chromatography. 15 μL aliquots of the reaction mixture were spotted onto Polygram TLC plates and developed with ascending chromatography in 100 mM phosphate buffer pH 7.0. The plates were scanned using a Typhoon (GE Healthcare) and analyzed with ImageQuant TL. Inhibition was tested by adding 200μM inhibitor to reaction solution. In addition, the reaction was performed using a 10 min pre-incubation of inhibitor and enzyme prior to substrate addition.

Molecular modeling—All molecular modeling steps utilized the Maestro Suite version 9.0 from Schrodinger Inc. The compounds **12** and **13** were protonated at the central linker nitrogen at pH 7, and a chiral centre exists at C6. Consequently, all possible stereoisomers were modeled and docked into the structure of BaDHPS obtained from the work of Kirk et al.5 The GlideXP module of Maestro was utilized for docking with only the highest scored pose retained for each molecule. The BaDHPS receptor structure for docking contained a conserved water molecule as shown in Figure 2c. The docking grid was generated with the centre of the box set to the centroid of the bound inhibitor in the BaDHPS structure in Kirk et al.5 and the box size was fixed by "dock with ligand length" option in Glide set to 15Å. Compound **11** was then redocked with the option to retain top 10 poses. The poses generated were visually inspected and best ranked pose was found to have a plausible binding mode. This was then subjected to 20 cycles of minimization using the Impact module with OPLS_2005 force field and all parameters set to default, followed by a 1 ns molecular dynamics simulation in vacuo using Impact with a time step of 1 fs, default OPLS_2005 force field and NVT constant temperature ensemble set to 298.15 K. Snapshots every 0.5 ps were recorded. All other parameters were left at their default values. For Figures 2a and 2b, crystal structures 1tww and 1tx0 respectively were used to reproduce figures 5 and 6 from Babaoglu et al..3

Acknowledgments

Cited literature

1. Domagk G. Ein Beitrag zur Chemotherapie der bakteriellen Infektionen. Dtsch Med Wochenschr. 1935; 61:250–253.

2. Achari A, Somers DO, Champness JN, Bryant PK, Rosemond J, Stammers DK. Crystal structure of the anti-bacterial sulfonamide drug target dihydropteroate synthase. Nat Struct Biol. 1997; 4:490–7. [PubMed: 9187658]

3. Babaoglu K, Qi J, Lee RE, White SW. Crystal structure of 7,8-dihydropteroate synthase from Bacillus anthracis: mechanism and novel inhibitor design. Structure. 2004; 12:1705–17. [PubMed: 15341734]

4. Baca AM, Sirawaraporn R, Turley S, Sirawaraporn W, Hol WG. Crystal structure of Mycobacterium tuberculosis 7,8-dihydropteroate synthase in complex with pterin monophosphate: new insight into the enzymatic mechanism and sulfa-drug action. J Mol Biol. 2000; 302:1193–212. [PubMed: 11007651]

5. Hevener KE, Zhao W, Ball DM, Babaoglu K, Qi J, White SW, Lee RE. Validation of Molecular Docking Programs for Virtual Screening against Dihydropteroate Synthase. J Chem Inf Model. 2009

6. Hevener KE, Yun MK, Qi J, Kerr ID, Babaoglu K, Hurdle JG, Balakrishna K, White SW, Lee RE. Structural studies of pterin-based inhibitors of dihydropteroate synthase. J Med Chem. 2010; 53:166–77. [PubMed: 19899766]

7. Nguyen JT, Hamada Y, Kimura T, Kiso Y. Design of potent aspartic protease inhibitors to treat various diseases. Arch Pharm (Weinheim). 2008; 341:523–35. [PubMed: 18763714]

8. Schramm VL, Horenstein BA, Kline PC. Transition state analysis and inhibitor design for enzymatic reactions. J Biol Chem. 1994; 269:18259–62. [PubMed: 8034566]

9. Hampele IC, D'Arcy A, Dale GE, Kostrewa D, Nielsen J, Oefner C, Page MG, Schonfeld HJ, Stuber D, Then RL. Structure and function of the dihydropteroate synthase from Staphylococcus aureus. J Mol Biol. 1997; 268:21–30. [PubMed: 9149138]

10. Ho MC, Shi W, Rinaldo-Matthis A, Tyler PC, Evans GB, Clinch K, Almo SC, Schramm VL. Four generations of transition-state analogues for human purine nucleoside phosphorylase. Proc Natl Acad Sci U S A. 2010; 107:4805–12. [PubMed: 20212140]

11. Winchester B, Fleet GW. Amino-sugar glycosidase inhibitors: versatile tools for glycobiologists. Glycobiology. 1992; 2:199–210. [PubMed: 1498417]

12. Fanta PE. Sodium Nitromalonaldehyde Monohydrate - Malonaldehyde, Nitro, Sodium Derivative. Organic Syntheses. 1952; 32:95–96.

13. Bernetti R, Mancini F, Price CC. Pyrido[2,3-D]Pyrimidines from Malonaldehydes. Journal of Organic Chemistry. 1962; 27:2863.

14. Taylor EC, Ray PS. Pteridines .51. A New and Unequivocal Route to C-6 Carbon-Substituted Pterins and Pteridines. Journal of Organic Chemistry. 1987; 52:3997–4000.

15. Singh SK, Dev IK, Duch DS, Ferone R, Smith GK, Freisheim JH, Hynes JB. Synthesis and biological evaluation of 5-deazaisofolic acid, 5-deaza-5,6,7,8-tetrahydroisofolic acid, and their N9-substituted analogues. J Med Chem. 1991; 34:606–10. [PubMed: 1995883]

16. Friesner RA, Banks JL, Murphy RB, Halgren TA, Klicic JJ, Mainz DT, Repasky MP, Knoll EH, Shelley M, Perry JK, Shaw DE, Francis P, Shenkin PS. Glide: a new approach for rapid, accurate docking and scoring. 1. Method and assessment of docking accuracy. J Med Chem. 2004; 47:1739–49. [PubMed: 15027865]

17. Luckner SR, Liu N, am Ende CW, Tonge PJ, Kisker C. A slow, tight binding inhibitor of InhA, the enoyl-acyl carrier protein reductase from Mycobacterium tuberculosis. J Biol Chem. 2010; 285:14330–7. [PubMed: 20200152]

18. Walter RD, Konigk E. 7,8-Dihydropteroate-synthesizing enzyme from Plasmodium chabaudi. Methods Enzymol. 1980; 66:564–70. [PubMed: 7374502]
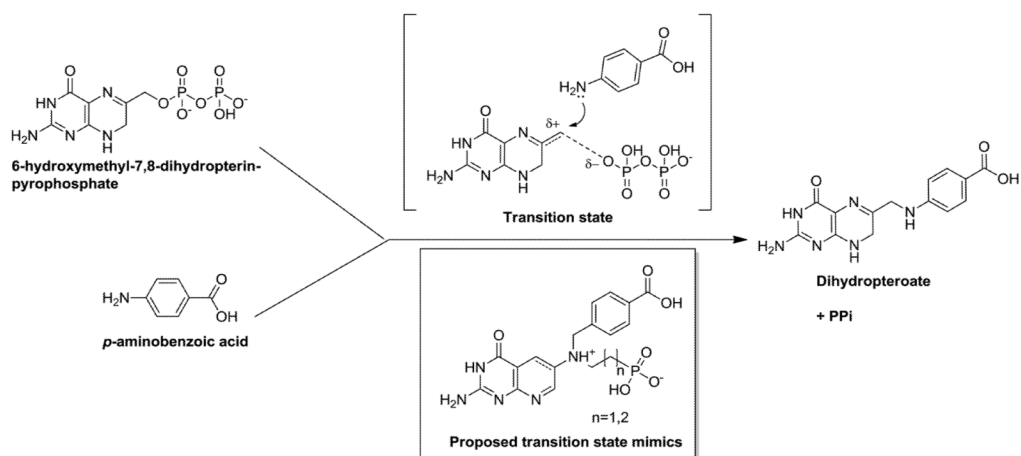
Figure 1.
DHPS catalytic reaction, proposed transition state intermediate and designed transition state mimics.
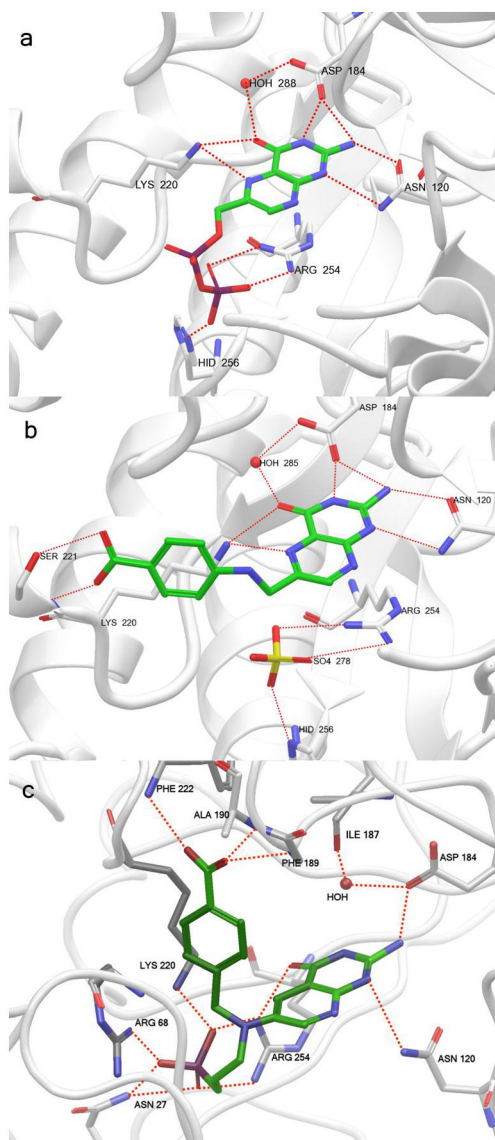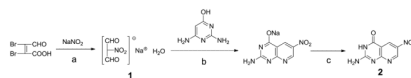
Figure 2.
Models of BaDHPS active site showing substrate, product and inhibitor binding: A, Model of the crystal structure of DHPP bound to the DHPS active site; B, Model of the crystal structure of product pteroic acid bound to DHPS; C, A snapshot taken at 1 ns of the MD simulation run on the docked complex of **11** and BaDHPS.

Scheme 1.
Reagents and conditions: (a) NaNO$_2$, H$_2$O, 54 °C, 1.5 h; (b) NaOH 1% aq, refluxed, 1 h; (c) 20%HCL.
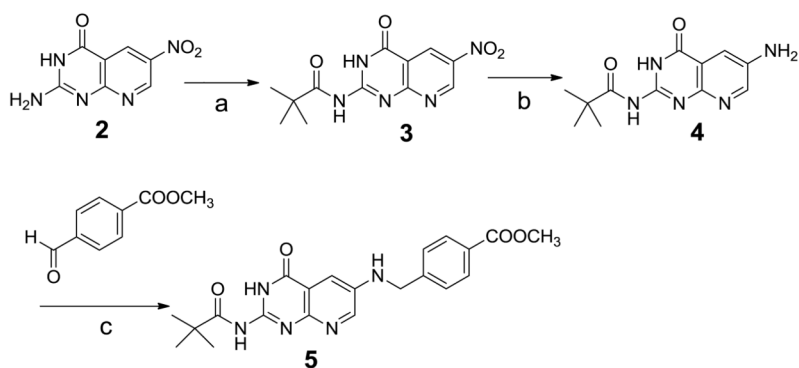
Scheme 2.
Reagents and conditions: (a) DMAP, pivaloyl anhydride, refluxing 6 h; (b) H_2 50 Psi/5%Pd-C, 2-methoxy-ethanol, RT, 3 h or Fe-AcOH, EtOH refluxing 2 h; (c) 1) AcOH, 4-formyl-benzoic acid methyl ester, RT, overnight; 2) borane-*tert*-butylamine complex.
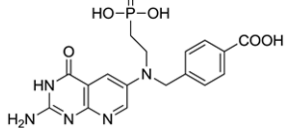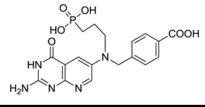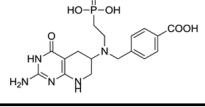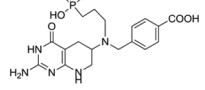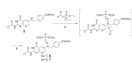
Scheme 3.
Reagents and conditions: (a) AcOH, RT, overnight; (b) borane-*tert*-butylamine complex

Scheme 4.
Reagents and conditions: (a) TMSBr, dry DCM, RT, 24 h; (b) H_2-PtO_2/50Psi, TFA, RT, 18 h; (c) 1.5M KOH/MeOH (1/1), RT, 24 h; (d) 1) 1N NaOH, RT, overnigh; 2) 1N HCL.

Table 1

BaDHPS inhibition by the designed inhibitors

	Structure	% Inhibition Activity (without pre-incubation)	% Inhibition Activity (with 10min pre-incubation*)
10		16.3@200μM	30.5@200μM
11		32.9@200μM	44.3@200μM
12		3.6@200μM	5.7@200μM
13		3.9@200μM	6.3@200μM

*
for pre-incubation, enzyme was incubated with inhibitor at 37°C for 10 min. Reaction was started by adding substrates.

Table 2

Glide docking scores for the synthesized inhibitors

Compound	Chirality at C	Chirality at N	Docking score
11			−6.93
12	S	R	−6.85
10			−6.55
12	S	S	−6.43
13	R	R	−6.27
13	S	S	−5.90
12	R	S	−5.70
13	R	S	−5.40
13	S	R	−5.33
12	R	R	−4.59